Applied Catalysis B: Environmental 98 (2010) 193–203

Contents lists available at ScienceDirect

Applied Catalysis B: Environmental

journal homepage: www.elsevier.com/locate/apcatb

New approaches to preferential CO oxidation over noble metals

Mikhail Kipnis*, Elvira Volnina

A.V. Topchiev Institute of Petrochemical Synthesis RAS, 29 Leninsky Prospect, 119991 Moscow, Russia

ARTICLE INFO

Article history:
Received 20 January 2010
Received in revised form 21 May 2010
Accepted 28 May 2010
Available online 4 June 2010

Keywords:
Preferential CO oxidation
Surface ignition
Platinum-group metals
Gold
Strong adsorption

ABSTRACT

Features of preferential CO oxidation (CO-PROX) over alumina-supported Pt-, Rh-, Ru-, Au-catalysts are investigated. As found in experiments (flow reactor of quartz, hydrogen-containing gas with admixtures of CO, $O_2 \sim 1$ vol.%, high gas flow rate), the nature of CO-PROX is found to be governed by a combination of two main decisive factors: high exothermicity of reactions (CO, H_2 oxidation), and peculiarities of interaction of reaction mixture components with metal. Due to high exothermicity, CO-PROX can be realized in a special macrokinetic mode, catalyst surface ignition (CSI), which is an external mass transfer control regime on O_2 as the key component.

The reaction can be transferred into CSI mode either by heating up to the critical temperature of ignition or by feeding the reaction gas to the catalyst at temperatures above the critical value. In heating, the transition into CSI mode starts with an overheat of the catalyst downstream, after which "hot spot" of the reaction drifts upstream. Variations of temperature allow to observe both ignition and extinction of catalyst surface.

Experiments performed with gas mixtures of different composition showed that in CO absence from the reaction gas, H_2 is easily oxidized over Pt and Rh at rather low temperatures close to a room one; reaction proceeds in CSI mode with the "hot spot" at the top of the catalyst bed. In CO-PROX over Pt, Rh, there is a deactivating effect of strong CO adsorption, while for Ru it is strong O_2 adsorption. As in the case of Ru-catalysts, hydrogen makes substantial positive effect on CO oxidation over Au-catalysts.

Effects of temperature, O_2 content in gas, Rh content in catalysts are investigated. It is found that a decrease in residual CO content in CSI mode is favored by higher O_2 content, lower temperature and lower metal content (for example, down from 1 to 0.2 wt.%).

1. Introduction

Studies of preferential CO oxidation (CO-PROX) started in 1960s with the purpose of pre-treating the reaction gas of ammonia synthesis [1,2]. Currently, the main purpose of such research is purification of hydrogen intended for use in PEM fuel cells, platinum anodes of which are poisoned by CO.

The process of catalytic CO oxidation to CO_2 (CO-PROX if in H_2 presence) is efficient enough and is studied intensively, in particular, over systems based on noble metals of Group VIII and gold [1–23].

One of the possible applications for fuel cells is automotive transport. The main requirement for a (quite compact by definition) unit of hydrogen generation/purification is sufficiently high throughput. This leads to an incentive for the development of a highly active and selective catalyst of CO-PROX.

According to calculations in [5], a ~20 kW fuel cell would require a throughput up to 400 l/min of moist gas generated in the process of methanol steam reforming. Hydrogen content in such gas is ~70%. Thus, for a ~100-kW powerful car at the catalyst loading volume ~1 l the space volume rate should be estimated as no less than 120 Nl (ml cat.)$^{-1}$ h^{-1}. A throughput this high at significant content of oxygen in gas leads to substantial release of heat, because the reactions of CO, H_2 oxidation are highly exothermic.

Correspondingly, for the reactions where the positive heat flow created by reaction surpasses the negative heat flow (heat dissipated from the reaction zone), a situation may arise where the reaction is transferred spontaneously into the external mass transfer control regime, resulting in a significant increase in temperature. This phenomenon has been called the catalyst surface ignition (CSI) by Frank-Kamenetskii, and the minimal temperature of catalyst at which ignition is possible, the *critical temperature of ignition* [24].

Ignition (and correspondingly, extinction) of the surface of Pt-, Rh-catalysts in CO oxidation has been observed in a number of publications: during stepwise heating/cooling over Rh/SiO_2 [25]; over honeycomb Pt-catalysts in linear heating/cooling [26,27] and in stepwise variation of O_2 concentration in initial mixture [27,28].

In several cases, a small change in temperature led in certain situations to rapid growth of CO conversion in CO-PROX over a Pt-

* Corresponding author. Tel.: +7 495 9541395; fax: +7 495 6338520.
E-mail address: kipnis@ips.ac.ru (M. Kipnis).

0926-3373/$ – see front matter © 2010 Elsevier B.V. All rights reserved.
doi:10.1016/j.apcatb.2010.05.029

and a Rh-catalyst ([3,17] correspondingly). The authors connected the observed phenomenon with ignition. Still, possible changes in temperature profile of catalysts and the role of ignition in these experiments, as a rule, were not researched in the mentioned works.

On the other hand, CO or O_2 are able to chemisorb strongly over some metals even in the presence of hydrogen. For example, strong adsorption of CO over Pt is demonstrated in [3,29,30], over Rh – in [31], while that of O_2 over Ru – in [16,32]. Positive effect of H_2 on CO-PROX over Au is associated by the authors of [18] with the proposition that hydrogen reacts with associatively adsorbed oxygen to yield highly oxidizing surface intermediates which convert CO to CO_2.

Despite a large number of works on CO-PROX over noble metals, the combination of its two main features, strong exothermicity of the reaction and deactivation caused by a reactant, as a rule, is not taken into consideration much.

In this work, features of CO-PROX in CSI mode are considered for Pt-, Rh-, Ru-, and Au-catalysts. Another important theme of discussion is the effect of strong adsorption of CO on the behavior of Pt-, Rh-catalysts.

Earlier, we have demonstrated in a flow reactor close to an adiabatic one the possibility of CO-PROX transition into the CSI mode. Features of such transition have been studied over a low-content Pt-catalyst (modified by Ru) [15] and Ru-catalysts [14,16,32].

For a study of reaction in CSI mode and the conditions allowing such mode, the experimental procedure was based on the monitoring: of catalyst bed temperature at two points, the entrance to the catalyst bed ("top") and the exit ("bottom"); also of residual CO content (with IR-analyzer), of residual O_2 content (GC analysis). Same procedure is applied to this study.

2. Experimental

2.1. Preparation of catalysts

Crushed commercial extrudates of γ-Al_2O_3 (Ryazan NPZ, Russia, type A-64k; specific surface 200 m^2/g; fraction 0.2–0.315 or 0.25–0.315 mm) were used for support. Alumina was calcined in air for 2 h at 500 °C before impregnation.

The catalysts were prepared by impregnation from aqueous solutions of $RuOHCl_3$, H_2PtCl_6, $RhCl_3{\cdot}3H_2O$, $HAuCl_4{\cdot}3H_2O$ at room temperature.

The desired amount of alumina was weighted, and then put into the aqueous solution of a given salt. In cases of Ru, Pt, Rh, the precursor was left in the solution for 20 h after stirring for 30 min. After the excess of liquid was decanted, the sample was dried for 6 h at 120 °C.

In synthesis of 1% Ru-catalyst, aqueous ammonia was added to the aqueous solution of $RuOHCl_3$ up to pH = 10 before the introduction of support.

In the case of Au-catalyst, the precursor was decanted directly after initial stirring (30 min) and dried at 90 °C. For removal of absorbed chlorine, this dried precursor was treated with aqueous ammonia (pH = 11) at stirring for 35 min. After decantation, the precursor was rinsed with distilled water several times till it became neutral, then it was dried at 72 °C for 17 h.

Reduction of catalysts was performed in the reactor.

In order to determine the conditions of activation for Pt-, Rh-, Au-precursors, they were heated in the mixture (vol.%: H_2 – 60, O_2 – 1, N_2 – balance) to the temperature of reduction after which the gas flow was switched to hydrogen. The value of oxygen conversion served as indicator of metal reduction.

Pt-catalyst was reduced in H_2 at 270 or 500 °C for 2 h; Rh-catalysts – 200 °C, 2 h; 0.1% Ru-catalyst – 350 °C, 2.5 h, 1% Ru-catalyst – 400 °C, 2 h.

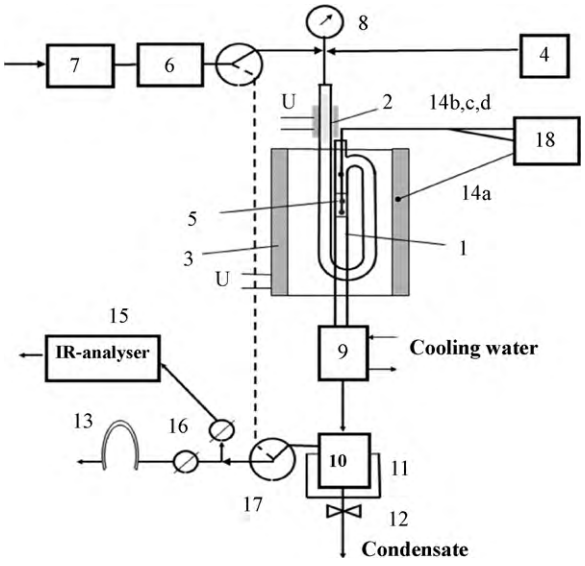

Fig. 1. Scheme of set-up for CO-PROX studies. 1 – reactor, 2 – evaporator, 3 – electric oven, 4 – water dosing device, 5 – catalyst, 6 – gas flow meter, 7 – gas flow regulating valve, 8 – manometer, 9 – cooler, 10 – separator, 11 – ice cooler (0 °C), 12 – cut-off valve, 13 – gas chromatograph, 14a–d – thermocouples, 15 – IR-analyzer, 16 – regulating valves, 17 – three-way valves, 18 – multichannel processor.

Au-catalyst was reduced in H_2 flow at 50 °C for 30 min, then heated up to 94 °C (oven temperature) in the flow of original reducing mixture (vol.%: H_2 – 60, O_2 – 1, N_2 – balance). After the level of oxygen conversion was almost complete, the catalyst was exposed at this temperature for ~1 h.

2.2. Gas mixtures

Initial gas mixtures were composed after preliminary evacuation of the gas cylinder and controlled by pressure of components. Special gas mixtures were composed for calibration and fine-tuning of IR-analyzer, in particular, for its CO channel – the bulk component was He or N_2, and CO content was in the range 8 ppm – 0.8 vol.% (Linde Gas/AGA, Balashikha Oxygen Plant).

2.3. Activity measurements

A flow set-up of scheme presented in Fig. 1 was used for catalytic studies. Quartz reactor 1 was of tubular form with prolonged inlet in order to heat the vapor–gas mixture at high flow rates (ID ~ 0.5 cm while that of the oven ~ 50 cm). Reaction gas was fed to the inlet 2 in the wall of reactor heated by an electric spiral. The inlet was packed with glass threads to accelerate evaporation. Thermal insulation of reactor zone inside the cylindrical electric oven 3 was ensured by ceramic plugs with holes for reactor inlet/outlet. Height of the catalyst bed at the loading 0.21–0.26 g was 1.3–1.6 cm. For the placing of catalyst loading 5, reactor 1 was fitted either with porous quartz insert soldered inside or with quartz matt insert. Catalyst was not diluted with inert packing in our experiments.

Two thin measuring thermocouples 14b and c (case OD = 0.1 cm, stainless steel) were inserted into the catalyst bed through a special reactor inlet with joint connection. Thermocouples were fixated within the metal part of the metal–glass connection. Their ends were placed within the catalyst bed in two key positions – at 0.1–0.2 cm from the entrance to the catalyst bed (top) and the exit (bottom).

In some cases, additional thermocouple 14d (placed at ~2.5 cm above the top) was used to measure the gas temperature above the catalyst bed (referred to as "gas temperature" hereafter).

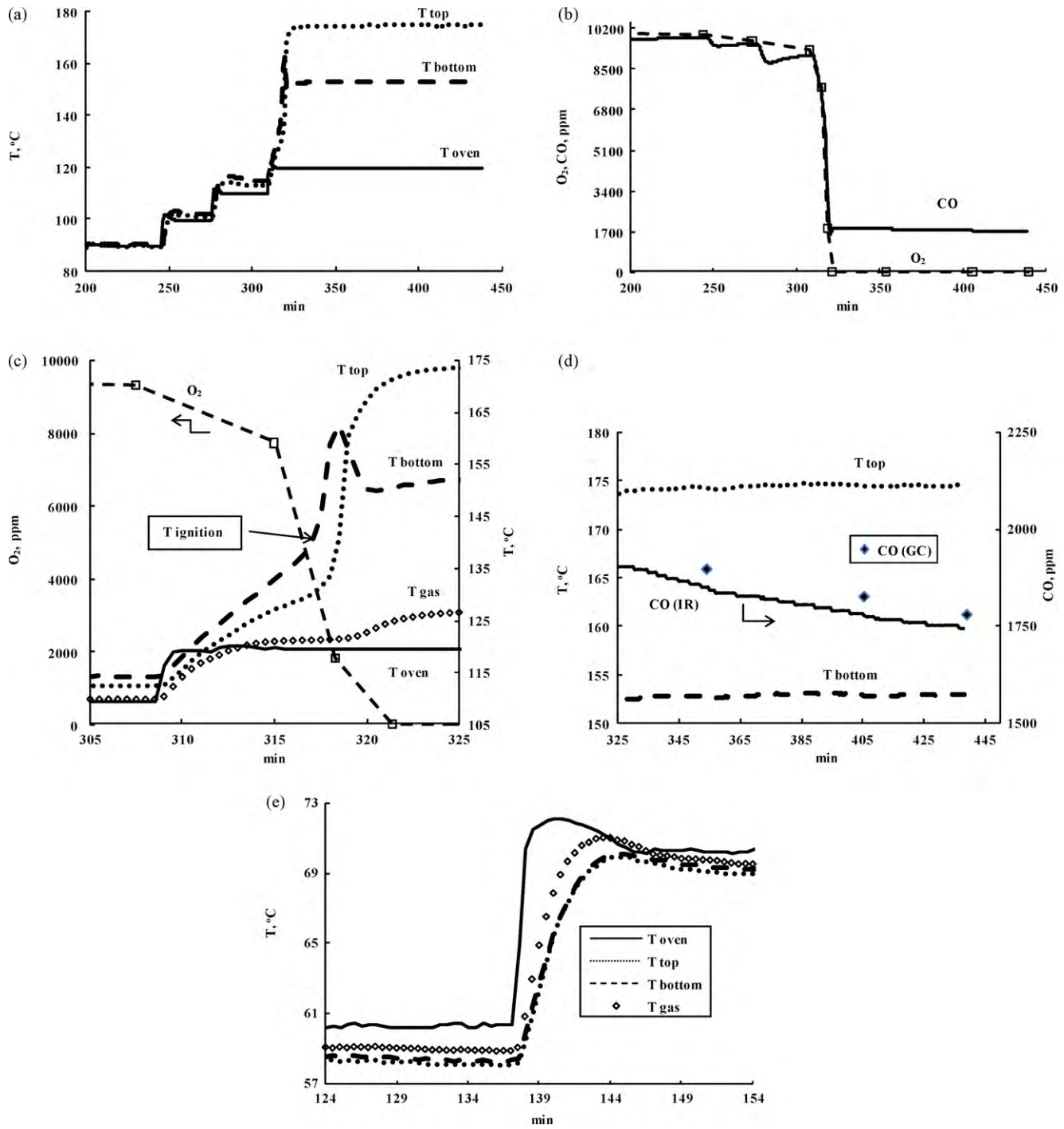

Fig. 2. Preferential oxidation of CO over 1% Rh/Al_2O_3. (a) The record of temperatures; (b) the record of residual contents (O_2, CO); (c) transition into the steady-state CSI on reaching *T* ignition at the bottom of catalyst bed; (d) drift in residual CO content in steady-state CSI (from data of IR-analyzer and chromatograph); (e) the record of temperatures at a single-step increase of oven temperature (in the absence of oxygen conversion). *T* oven, *T* top, *T* bottom, *T* gas – correspondingly, temperatures of: oven; top and bottom of catalyst bed; gas over the catalyst bed. Gas mixture composition, vol.%: O_2 – 1.02, CO – 1.02, H_2 – 60, N_2 – balance. GHSV 55 Nl (g cat.)$^{-1}$ h^{-1}.

Oven temperature was controlled by thermocouple 14a placed near the electric spiral in the oven case and connected to processing unit 18.

Within the temperature range of experiments the temperature gradient along the layer was less than ~1 °C in the absence of reaction, and the catalyst bed temperature was not that different from the temperature measured by the controlling thermocouple.

Gas flow rate was set by controlling valve 7 and measured by digital meter 6 (discreteness 1 ml/min), the final value was calculated for normal conditions (760 torr, 0 °C). Excessive pressure in the reactor was shown by manometer 8. As a rule, it did not exceed 0.02 MPa.

Water was condensed at the reactor exit (in the cases where initial gas contained some) first in cooler 9 then in separator 10 placed into ice cooler 11. Condensate was retrieved through valve 12.

Dried gas (0 °C) was split in two streams after the separator by precision valves 16: one for the chromatographic and another, the

main one, for IR analysis. Most of experiments described in this work were done without adding water to the reaction gas; accordingly, parts 4, 9–12 were shut off most of the time.

GC analysis was performed on CO, CH_4, O_2 (TCD, zeolite 13 X). Content of CO and CO_2 was monitored by 2-channel IR-analyzer BINOS 100 (CO channel: range 0–9999 ppm, discreteness 1 ppm; CO_2 channel: range 0–25 vol.%, discreteness 0.1 vol.%). Analog signal of IR-analyzer was put into processor 18.

Before the experiment, the reactor was made gas-tight then heated in flow of hydrogen up to the temperature of experiment. When needed, water was fed into the evaporator. Then H_2 flow was switched to that of reaction gas with 5-position Swagelok switch. After the experiment the reactor was flushed with hydrogen and shut off with 3-position switches 17, so the catalyst stayed in hydrogen atmosphere.

The error in CO concentration measured in gas was determined by the errors in preparation of calibration gas mixtures. At small contents of CO (~20 ppm and less) it did not exceed 1–2 ppm. It should be mentioned that the input of CO_2 into the signal generated in CO channel was duly noted in data processing.

2.4. Calculations of the reaction activity and selectivity

O_2 and CO conversion values were calculated from the area of corresponding chromatographic peaks (small changes in gas space velocity connected to H_2 and CO transformation were neglected). Selectivity of O_2 consumption in CO oxidation was calculated as (1):

$$S = 0.5 \times C^{\circ}_{CO} \times \frac{X_{CO}}{(C^{\circ}_{O_2} \times X_{O_2})}, \quad (1)$$

where X_{CO}, X_{O_2} – conversion of CO, O_2; $C^{\circ}_{CO}, C^{\circ}_{O_2}$ – initial concentration of CO, O_2.

3. Results

3.1. Reaction transition into CSI mode at the increase in oven temperature

3.1.1. Rh/Al_2O_3

Let us consider reaction transition into CSI mode at the increase in oven temperature with 1% Rh/Al_2O_3 catalyst as the example (Fig. 2). Hydrogen was fed at room temperature into the reactor loaded with preliminarily reduced catalyst, after which the temperature was increased up to 50 °C and H_2 was switched to the gas mixture of the following composition (vol.%): O_2 – 1.02, CO – 1.02, H_2 – 60, N_2 – balance. After this, oven temperature was increased in 10 °C steps. When it reached 120 °C, a temperature jump in the catalyst bed was observed (Fig. 2a), accompanied by rapid fall of residual O_2, CO contents (Fig. 2b). These sudden changes are better illustrated in Fig. 2c. An increase in oven temperature at 309 min caused gradual increase in temperature in the catalyst layer observed until (circa) 317 min. It is seen that temperature of the bottom was higher than that of the top – thus, the reaction occurred mainly at the bottom, at the exit from the catalyst layer.

Then, for 1.5 min the bottom temperature grew by 20 °C and decreased after passing through a maximum (318.5 min). At the same time, the top temperature grew quickly, achieving 173.6 °C at 325 min. Notice that the bottom temperature at this moment was just 152.2 °C. Before the heating (up to 120 °C) was started at 309 min, it was higher than the oven temperature only by 4.5 °C.

The observed phenomenon can be interpreted thus: starting from 317 min, when the value of the critical temperature of ignition (*T* ignition) was reached at the bottom of catalyst bed, transition of reaction into CSI mode was witnessed.

Significant heat effect observed in this experiment affected the gas temperature which grew starting from circa 319 min (Fig. 2c). This is explained by gradual heating of reactor walls due to exothermic reactions of oxidation which occur at the top. Starting from circa 325 min, the system was at what may be considered a steady temperature level of the catalyst bed (Fig. 2a), so the residual O_2 content was constant as well (Fig. 2b). At the same time, there was some declining trend in residual CO content, recorded both by IR and GC units (Fig. 2d) (Step-like irregularities in the curves recorded by IR-analyzer depended on the characteristics of the processor.).

This slow decrease in residual CO content at almost full oxygen consumption points at the growth of CO oxidation input into consumption of oxygen. Probably, this decrease happens due to the ongoing surface restructuring of metal crystallites.

It should be noted that in the absence of CSI mode, a new steady state can be established in circa ~15 min after the increase in oven temperature, both in catalyst bed and in gas (Fig. 2e).

3.1.2. Ru/Al_2O_3

Fig. 3 illustrates the reaction transition into CSI mode in heating of 1% Ru/Al_2O_3 catalyst for the following gas mixture (vol.%): O_2 – 0.97, CO – 0.98, H_2 – 60, N_2 – balance. As in the case of Rh, gradual increase in oven temperature leads first to an overheat of catalyst at the bottom, then at the top (Fig. 3a). In this, corresponding changes in residual O_2, CO content were observed, as well as CO_2 formation (Fig. 3b). Transition into CSI mode as such is depicted in Fig. 3c: sharp increase in temperature at the bottom starts after the critical temperature (*T* ignition) is achieved, and the steady state of CSI is established fully in ~16 min after the establishment of steady temperature regime in the oven. Unlike in 1% Rh/Al_2O_3 case (Fig. 2), over 1% Ru/Al_2O_3 in CSI mode the residual CO content is at the constantly low level of ~120 ppm.

3.2. Reaction transition into CSI mode after feeding the reaction gas above the critical temperature of ignition

3.2.1. Au/Al_2O_3

If the reaction gas is fed into reactor when temperature at the entrance to the catalyst bed (the top) is higher than *T* ignition, transition into CSI mode begins at the top.

This is illustrated in Fig. 4 for 1% Au/Al_2O_3 catalyst at the switch from H_2 to gas mixture of composition (vol.%): O_2 – 1.02, CO – 1.02, H_2 – 60, N_2 – balance. A change in feed gas led to a quick increase in temperature, first of all at the top. In circa 10 min, steady CSI mode was established. In this, temperature at the top exceeded that before the experiment by ~59 °C (Fig. 4a) and residual O_2 was ~30 ppm, residual CO content was ~2700 ppm (Fig. 4b). This increase in the top temperature caused by the reaction has led to overheat of reactor walls as well resulting in a growth of gas temperature by ~9 °C (Fig. 4a).

High value of residual CO content (~2700 ppm, Fig. 4b) is explained in this case by non-optimal conditions of the reaction (temperature, gas flow rate, O_2/CO ratio, metal loading in the catalyst). After the flow of a H_2-containing mixture is switched to that of a similar mixture lacking H_2, the reaction practically stopped: temperature of the catalyst bed decreased first quickly, then at a slower rate (Fig. 4a), while residual contents of O_2, CO at the reactor exit grew monotonously approaching their initial values (Fig. 4b). Thus, in hydrogen absence CO oxidation proceeds to a much smaller degree.

At the same time, a switch from $H_2/O_2/N_2$ to $H_2/O_2/CO/N_2$ did not lead in our experiments to changes in the macrokinetic mode of the reaction. The macrokinetic mode of the reaction did not change, as can be understood from two moments: such switch does not affect the placement of "hot spot" (it is still at the top); residual O_2 content is unchanged, remaining at the level ~30 ppm.

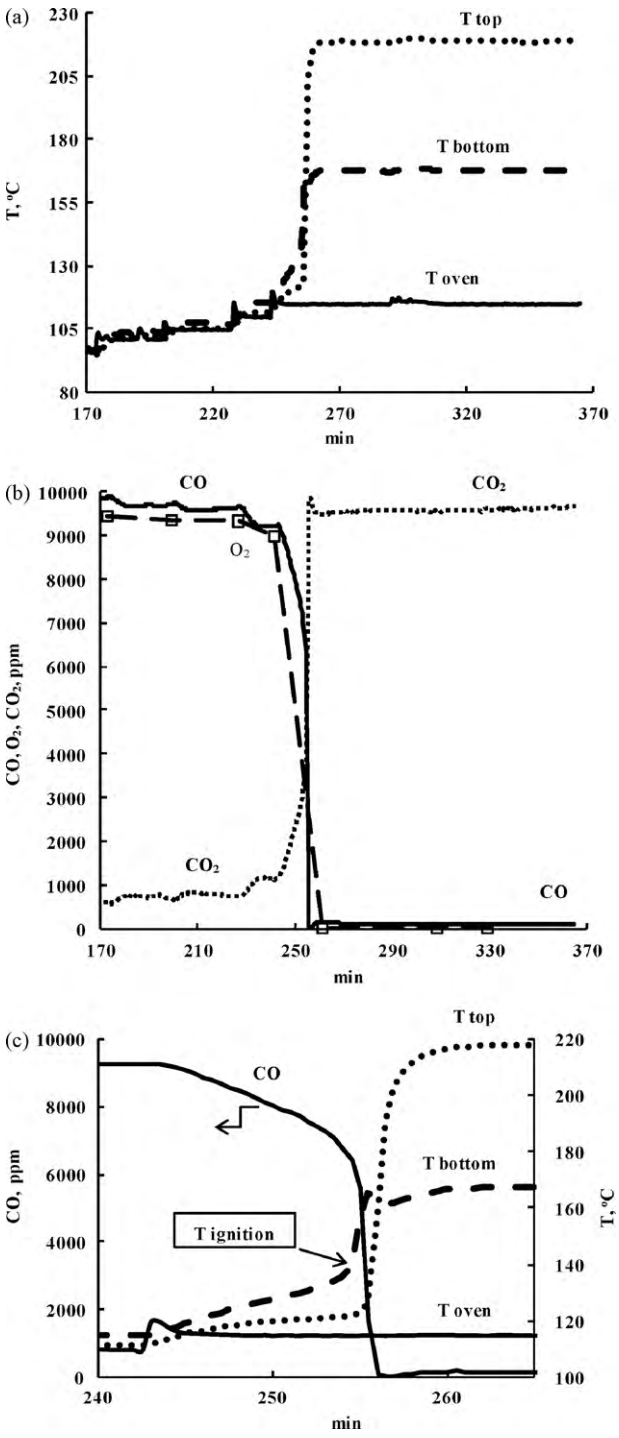

Fig. 3. Preferential oxidation of CO over 1% Ru/Al_2O_3: transition into CSI mode and establishment of steady-state CSI. (a) The record of temperatures; (b) the record of residual contents (O_2, CO) and of CO_2 content; (c) transition into the steady-state CSI on reaching *T* ignition at the bottom of catalyst bed. *T* oven, *T* top, *T* bottom – correspondingly, temperatures of: oven; top and bottom of catalyst bed. Gas mixture composition, vol.%: O_2 – 0.97, CO – 0.98, H_2 – 60, N_2 – balance. GHSV 79 Nl (g cat.)$^{-1}$ h^{-1}.

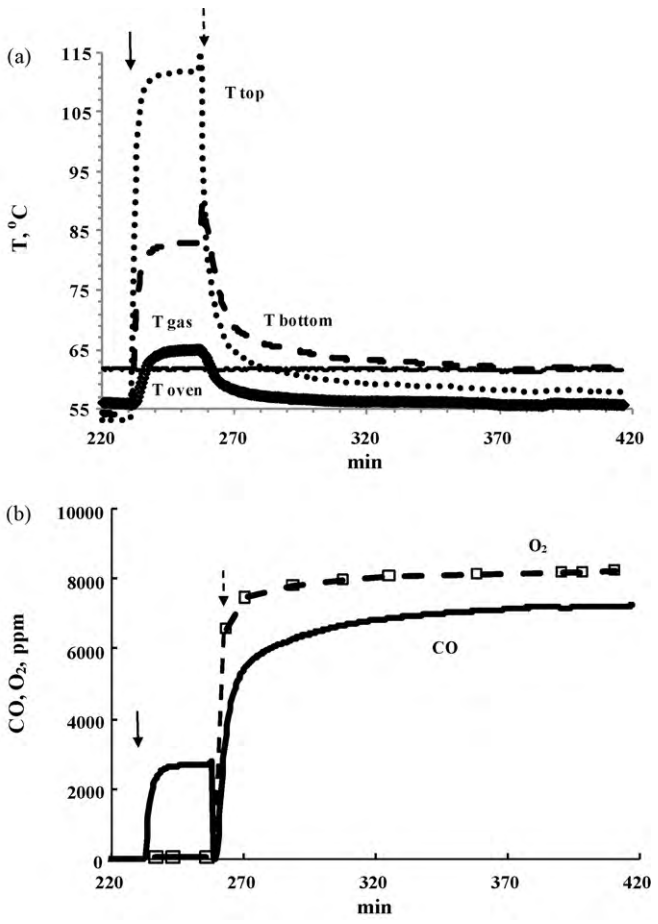

Fig. 4. Effect of hydrogen on CO oxidation over 1% Au/Al_2O_3: transition into the CSI mode at the change of feed gas from H_2 to the gas mixture (composition, vol.%: O_2 – 1.02, CO – 1.02, H_2 – 60, N_2 – balance) – marked by a solid arrow. Dashed arrow marks the change to another, hydrogen-free gas mixture (composition, vol.%: CO – 0.96, O_2 – 0.97, N_2 – balance). (a) The record of temperatures; (b) the record of residual contents (O_2, CO). *T* oven, *T* top, *T* bottom, *T* gas – correspondingly, temperatures of: oven; top and bottom of catalyst bed; gas over the catalyst bed. GHSV 38 Nl (g cat.)$^{-1}$ h^{-1}.

Thus, as in the case of Au, so in that of Ru [16,32], interaction of hydrogen and oxygen is important for CO-PROX to proceed. The positive effect of H_2 in CO oxidation is reflected in the mechanism which proposes formation of a number of H_2–O_2-containing intermediates over Au [33]. Slow gradual change in products composition at a change in reaction conditions has been observed also in the case of Pt and ascribed to the establishment of a new equilibrium in the system [3]. It is also our viewpoint that in our case, a slow decrease in residual contents of O_2, CO in a switch to H_2-free gas reflects the establishment of a new equilibrium in the system.

3.2.2. Ru/Al_2O_3

In the case of 0.1% Ru/Al_2O_3 catalyst, Fig. 5 illustrates reaction transition into CSI mode at the entrance to the catalyst bed (the top) after switching H_2 to the gas mixture (composition, vol.%: O_2 – 0.75, CO – 0.76, CO_2 – 19, H_2 – 56, H_2O – 20, N_2 – balance). After establishment of steady-state CSI residual CO concentration leveled at ~3900 ppm, while that of O_2 – at ~20 ppm.

Gradual decrease in oven temperature from 299 to 170 °C did not change the reaction mode: at the top, it was still CSI. Further decrease led to the drift of "hot spot" from the top to the bottom. Thus, starting from 335 min, temperature at the bottom became higher than that at the top, i.e. the extinction of surface has started. When the bottom temperature achieved ~225 °C, the extinction set in after ~383 min: residual contents of O_2, CO returned to levels close to the initial ones (at 409 min).

It should be noted that in CSI mode, right down to its extinction, temperature decrease did not affect residual O_2 content in any way: the reaction proceeded in external mass transfer control regime in regard to oxygen. Nevertheless, the changes in residual CO content were quite significant, as seen from Fig. 5. Thus, in the case of a

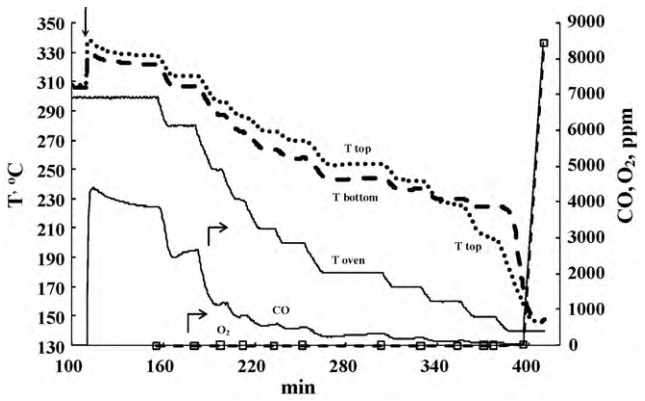

Fig. 5. Preferential oxidation of CO over 0.1% Ru/Al_2O_3: transition into the CSI mode at the change of feed gas (marked by an arrow) from H_2 to the gas mixture (composition, vol.%: O_2 – 0.75, CO – 0.76, H_2 – 56, CO_2 – 19, H_2O – 20, N_2 – balance) and work in CSI mode during cooling. *T* oven, *T* top, *T* bottom – correspondingly, temperatures of: oven; top and bottom of catalyst bed. GHSV 92 Nl (g cat.)$^{-1}$ h^{-1}.

Ru-catalyst, a temperature decrease in CSI mode leads to a growth in selectivity on oxygen consumption.

Rather low values of residual CO content (below 200 ppm) were obtained in this case at high space velocity (92 Nl (g cat)$^{-1}$ h^{-1}) and high content of CO_2 and H_2O in initial gas.

3.3. CSI mode and hysteresis phenomenon

Surface ignition during the temperature rise and surface extinction at the cooling can be demonstrated for the example of 0.2% Rh/Al_2O_3 catalyst (Fig. 6).

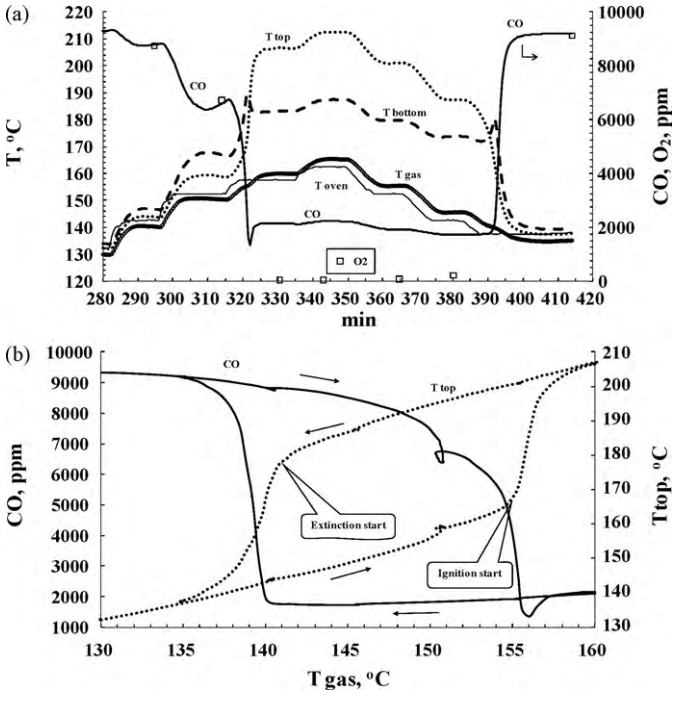

Fig. 6. Preferential oxidation of CO over 0.2% Rh/Al_2O_3: hysteresis during heating and cooling. (a) Dynamics; (b) hysteresis loop for temperature of the top of catalyst bed (*T* top) and residual CO content as plotted against the gas temperature over the catalyst bed (*T* gas) – arrows depict the dynamics of gas temperature. *T* oven, *T* top, *T* bottom, *T* gas – correspondingly, temperatures of: oven; top and bottom of catalyst bed; gas over the catalyst bed. Gas mixture composition, vol.%: O_2 – 0.97, CO – 0.97, H_2 – 62, N_2 – balance. GHSV 47 Nl (g cat.)$^{-1}$ h^{-1}.

In the range 315–325 min, heating of catalyst in the gas mixture (vol.%: O_2 – 0.97, CO – 0.97, H_2 – 62, N_2 – balance) led to the establishment of CSI mode accompanied by corresponding sudden growth of temperatures at the top and bottom of catalyst layer and the decrease in residual O_2 content down to ~40 ppm (Fig. 6a). Subsequent variations of oven temperature did not affect the established mode until the temperature of the top fell below the critical value (at ~384 min), after which the "hot spot" drifted to the bottom and the surface extinction occurred quickly. Its features were: corresponding drop in catalyst bed temperature (top, bottom) and growth in residual O_2 content almost to its initial level (414 min). Residual CO content underwent similar changes: it decreased during the transition into CSI mode only to return almost to the initial level during surface extinction.

In this, changing values of temperature at the top and of residual CO concentration are shown to form hysteresis loops depending on gas temperature (Fig. 6b). An increase in gas temperature first leads to monotonous growth in temperature at the top, up to the critical temperature of ignition. Then surface ignition occurs in a narrow range of gas temperature, and temperature at the top grows rapidly – there is the transition from the lower to the upper part of the hysteresis loop. When temperature is decreased further, the monotonous decrease in temperature at the top is observed until the critical temperature of extinction is reached. After this, the return to the lower part of the hysteresis loop happens. Residual CO content undergoes through similar motions, the difference being in different direction, from above to below and back, and residual oxygen content follows the same pattern.

3.4. Oxidation of H_2 and CO-PROX over Pt

Effect of CO on oxidation of hydrogen over Pt is illustrated in Fig. 7, where the catalyst reduced at 270 °C was subjected at room temperature to alternating feeds of a gas mixture containing O_2, H_2, N_2 and another, CO, O_2, H_2, N_2.

Hydrogen is easily oxidized over Pt when the mixture with just O_2, H_2, N_2 is fed on. The moment when this mixture was switched on after reduction in hydrogen (Fig. 7a, 18 min) showed a sharp increase in catalyst temperature: ~107 °C at the top, ~69 °C at the bottom. In this, a decrease in oxygen content was detected at the exit – down to ~40 ppm (Fig. 7b). Thus, reaction of hydrogen oxidation proceeded in CSI mode at the top.

Appearance of CO in gas (at 36 min) led first to rapid, then to slow decrease in catalyst temperature (Fig. 7a). Repeated runs without CO (Fig. 7a, 53 and 134 min) and with CO (Fig. 7a, 66 and 175 min) reproduced the patterns already seen: catalyst heated up in gas mixture without CO and cooled down when CO was in the gas mixture. Thus, catalyst deactivated previously in contact with CO regained its activity quickly from the moment CO was excluded from the gas mixture – just like a freshly reduced sample (Fig. 7a and b).

The manner in which catalytic activity declines with time when CO is present in gas can be seen from Fig. 7c and d.

Residual CO content grew slowly with time after the change in gas composition (a delay less than 2 min should be mentioned for IR-analyzer), while catalyst temperature did otherwise (Fig. 7c). In Fig. 7d, conversion of oxygen is compared to half of that for CO. At equal concentrations of CO and O_2, the ratio of values mentioned above gives the selectivity of O_2 consumption in CO oxidation (1). As seen from the figure, the curves of O_2 conversion and half-value of CO conversion lay in close proximity, which gives selectivity ~1. This means that oxygen is consumed only in CO oxidation to CO_2 (appearance of CO_2 is confirmed by the data from the CO_2 channel of IR-analyzer).

In the cases when there was a rapid decline in temperature at the top after switching gas to CO-containing one, temperature at

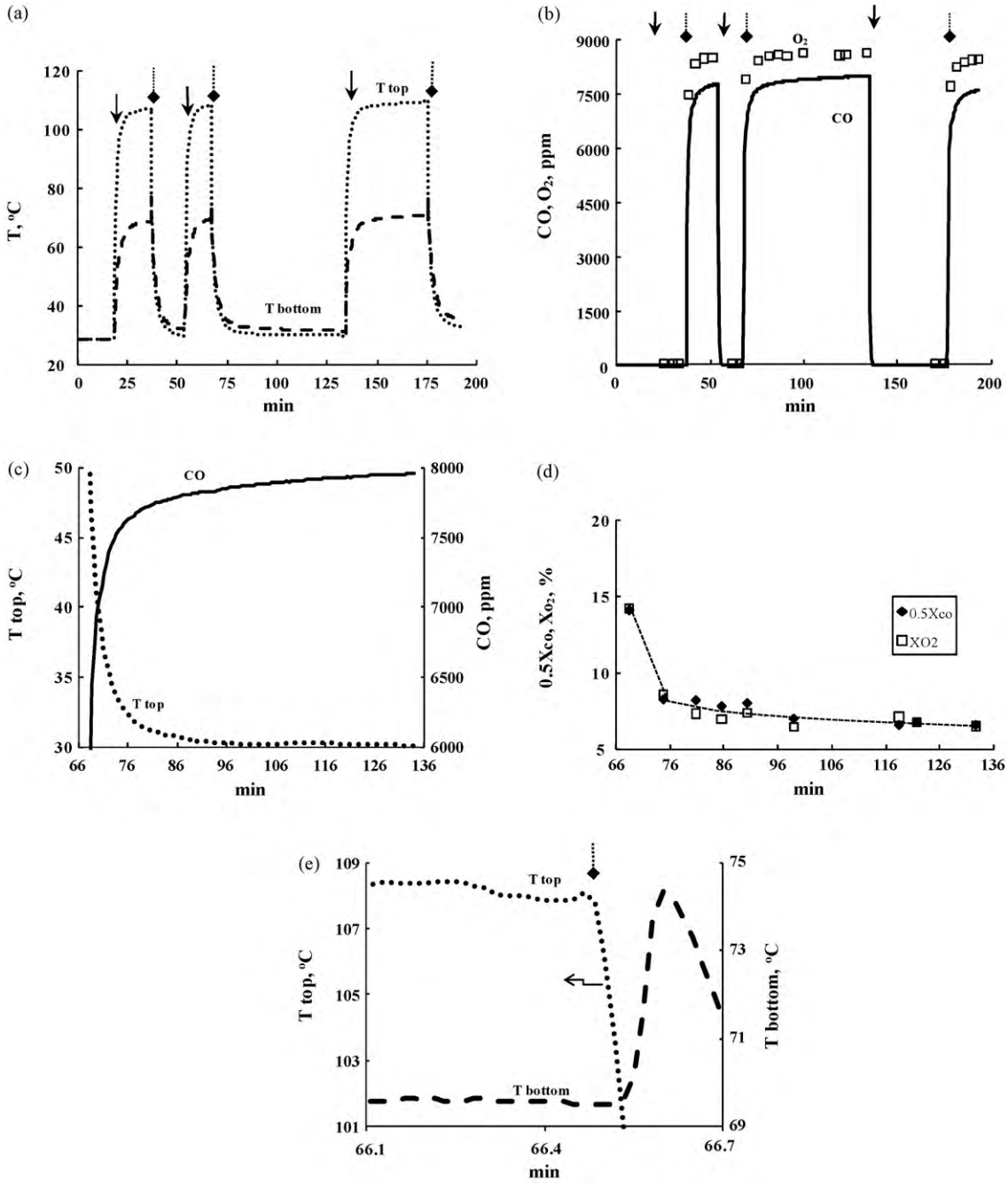

Fig. 7. Behavior of 1% Pt/Al_2O_3 catalyst (reduced at 270 °C) in alternating runs with gas mixtures: H_2, O_2, N_2 and CO, H_2, O_2, N_2. (a) Temperature dynamics in the catalyst bed; (b) dynamics of residual contents (O_2, CO); (c and d) the records made after switching at 66 min to a CO-containing gas mixture; (e) temperature dynamics in the catalyst bed after switching to a CO-containing gas mixture. *T* top, *T* bottom – correspondingly, temperatures of: top and bottom of catalyst bed; $0.5X_{CO}$ – halved value of CO conversion (♦), X_{O_2} – O_2 conversion (□). Solid arrows indicate the switching to the gas mixture composition, vol.%: O_2 – 1, H_2 – 60, N_2 – balance and the dotted arrows – the switching to the gas mixture composition, vol.%: O_2 – 0.92, CO – 0.93, H_2 – 62, N_2 – balance. GHSV 48 Nl (g cat.)$^{-1}$ h^{-1}.

the bottom went through a maximum. The delay between the start of temperature decline at the top and temperature maximum at the bottom was ~0.1 min (Fig. 7e).

This decrease in temperature at the top when CO is present in gas occurs due to strong adsorption of incoming CO on Pt which leads to gradual deactivation of the catalyst starting from the top. At the same time, as CO concentration decreases along the catalyst bed due to adsorption, O_2 is free to react with H_2, the further downstream the more intensely, so temperature at the bottom jumped up by 5 °C (Fig. 7e). Nevertheless, incoming CO deactivates the catalyst gradually, reaching the lower layers at the bottom.

Strong CO adsorption over Pt is essential below 200 °C [29,30], affecting in a certain way CO-PROX in a continuous catalyst bed even at high O_2 conversion. In order to highlight the role of CO at increased temperature, we used the sample with lowered activity (this was achieved by reduction not at 270 °C, but at 500 °C). Higher temperature of reduction produces a less active catalyst due to sintering of metal crystallites. For such catalyst, the input of strong CO adsorption is noticeable as early as at 200 °C (Fig. 8), but the proceeding of CO-PROX over it has some interesting peculiarities.

After a switch from H_2 to the gas mixture of (vol.%): O_2 – 0.96, CO – 0.96, H_2 – 71, N_2 – balance, an overheat of the catalyst hap-

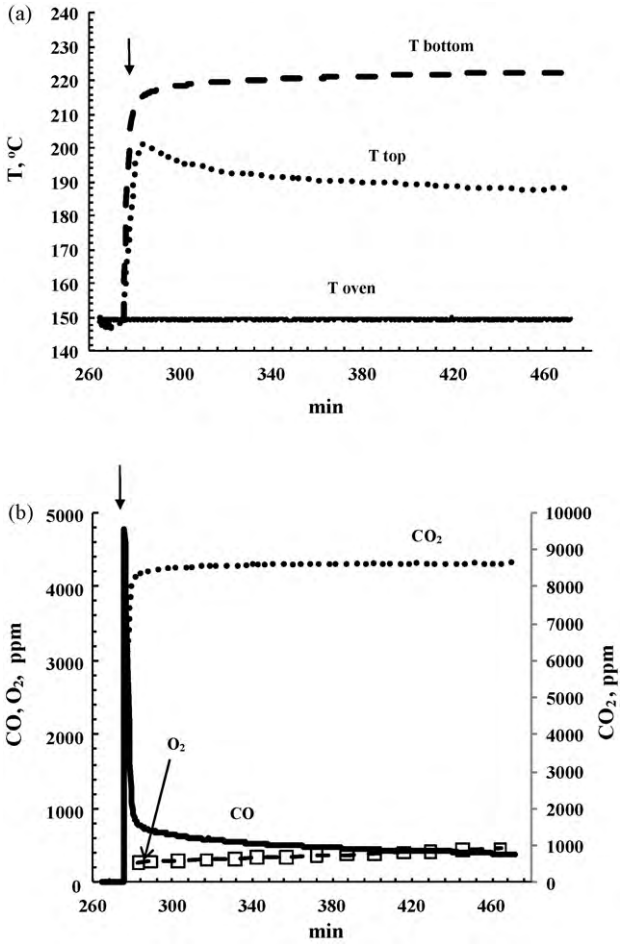

Fig. 8. Preferential oxidation of CO over 1% Pt/Al_2O_3 (reduced at 500 °C). (a) The record of temperatures; (b) the record of residual contents (O_2, CO) and CO_2. *T* oven, *T* top, *T* bottom – correspondingly, temperatures of: oven; top and bottom of catalyst bed. An arrow indicates the change of feed gas from H_2 to the gas mixture (composition, vol.%: O_2 – 0.96, CO – 0.96, H_2 – 71, N_2 – balance). GHSV 71 Nl (g cat.)$^{-1}$ h^{-1}.

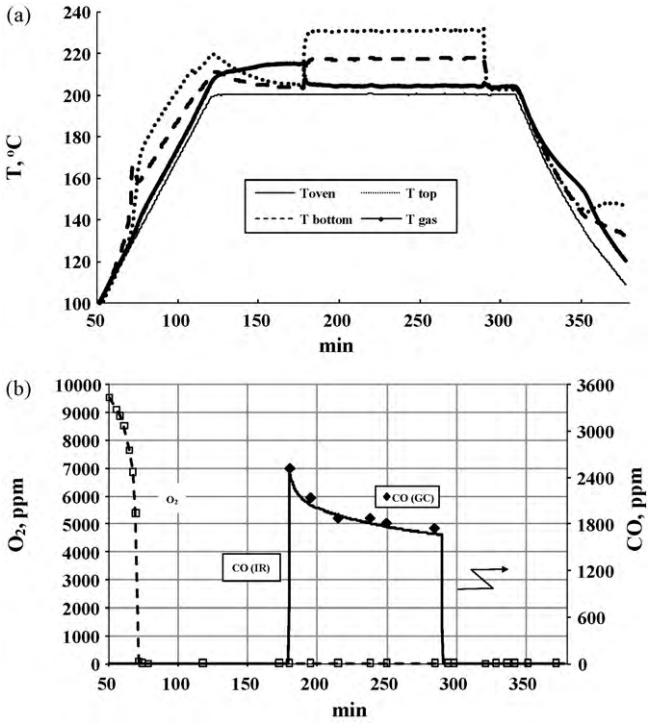

Fig. 9. Activation of 1% Rh/Al_2O_3 with subsequent selective oxidation of CO over the activated catalyst. The experiment was performed without the insertion of porous quartz matt above the catalyst bed. (a) The record of temperatures; (b) the record of residual contents (O_2, CO) (from data of IR-analyzer and chromatograph). *T* oven, *T* top, *T* bottom, *T* gas – correspondingly, temperatures of: oven; top and bottom of catalyst bed; gas over the catalyst bed. Up to 179 min and starting from 290 min the gas mixture composition was (vol.%): O_2 – 1, H_2 – 60, N_2 – balance. In the range 179–290 min the gas mixture composition was (vol.%): O_2 – 1.02, CO – 1.02, H_2 – 63, N_2 – balance. GHSV 33 Nl (g cat.)$^{-1}$ h^{-1}.

pened quickly first and foremost at the bottom (Fig. 8a) with the corresponding drop in residual contents of O_2, CO and also with appearance of CO_2 (Fig. 8b). Still, no upstream drift of the "hot spot" happened in this case, and residual oxygen content while remaining not significant (~300–400 ppm), nevertheless grew monotonously; accordingly, catalyst bed temperature grew at the bottom yet fell at the top. Such behavior of the catalyst testifies to the deactivating effect of strong CO adsorption. It is interesting that residual CO content declined monotonously all this time (Fig. 8b).

Similar phenomenon of deactivation below 200 °C was observed by us for Ru; the reason was strong adsorption of oxygen (for example [14,16]). Decreased catalytic activity at the top meant that the "hot spot" was situated at the bottom.

With regard to hydrogen oxidation and CO effect on it, reduced Rh-catalysts behave similarly [31].

3.5. Activation of Rh/Al_2O_3 catalyst and H_2 oxidation over Rh

As noted above (see Section 3.4), in CO absence hydrogen oxidizes easily over Pt and Rh at about room temperature. This allows to use conversion of O_2 in hydrogen-containing gas as the indicator of catalyst reduction. Thus, by using hydrogen with small admixture of O_2 for reduction of the catalyst precursor it is possible to evaluate the initial temperature of catalyst activation in linear heating mode.

Data which illustrate this are depicted in Fig. 9. Catalyst precursor was heated in the flow of gas mixture (composition, vol.%: O_2 – 1, H_2 – 60, N_2 – balance) with the increment of 1.4°/min. As seen from Fig. 9a and b (showing temperature and residual O_2 content, correspondingly), oxygen content was noticeably lower than its initial value at as low temperature of the bottom as 111 °C (58 min). Further heating gave way to rapid decrease in residual O_2 content (~110 ppm, 71.5 min – Fig. 9b) accompanied by an overheat of the catalyst bed, first of all at the bottom (Fig. 9a). In this, temperature of the bottom went through an extremum (71.5 min, Fig. 9a), after which the "hot spot" drifted to the top.

Thus, it can be said that the reaction of H_2 oxidation went into CSI mode at the top.

In an interesting turn of events, after CSI mode was established and while the oven temperature was at a constant level, a decrease in catalyst temperature (both at the top and the bottom) was observed, although gas temperature (measured above the top of catalyst, as described earlier) increased – see Fig. 9a. This phenomenon, a decrease in catalyst temperature at the increase in gas temperature, testifies unequivocally to reaction of hydrogen oxidation spreading out from the boundaries of catalyst bed. It ceased when CO was introduced to the gas (gas mixture composition, vol.%: O_2 – 1.02, CO – 1.02, H_2 – 63, N_2 – balance) at 179 min – see Fig. 9a. In this, temperature of the top jumped up quickly, while that of gas decreased almost to the level of oven temperature. Residual content of oxygen was ~30 ppm (Fig. 9b) and remained the same at further exposure to gas mixture with CO, typically for CSI. Still, residual CO content declined monotonously according both to GC and IR analyses (Fig. 9b). The effect of gradual decline in residual CO

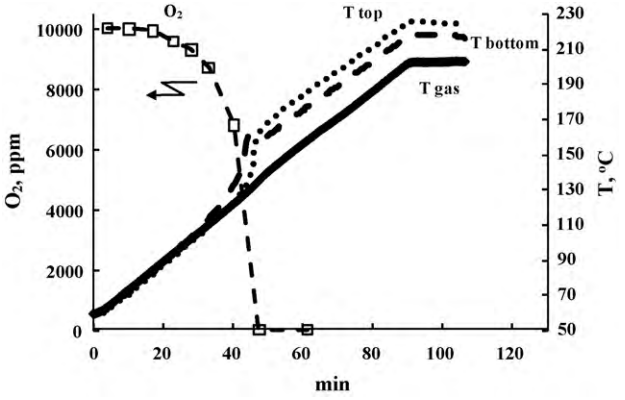

Fig. 10. Activation of 1% Rh/Al_2O_3. The experiment was performed with the insertion of porous quartz matt above the catalyst bed. *T* top, *T* bottom, *T* gas – correspondingly, temperatures of: top and bottom of catalyst bed; gas over the catalyst bed. Gas mixture composition, vol.%: O_2 – 1, H_2 – 60, N_2 – balance. GHSV 35 Nl (g cat.)$^{-1}$ h^{-1}.

content over a 1% Rh-catalyst in steady-state CSI was noted above in discussion of data shown in Fig. 2d.

At 290 min, gas was switched back to a feed without CO (vol.%: O_2 – 1.0, H_2 – 60, N_2 – balance). Although temperatures of both gas and catalyst became close to that of oven, i.e. no overheat happened because of reaction, hydrogen oxidation proceeded still in the reactor, as detected by low value of residual O_2 content (Fig. 9b). It was concluded that once more, the reaction did not limit itself to catalyst bed.

When reactor was cooled, it became possible to observe the shrinking of reaction zone from its expanded domain (catalyst bed and gas phase above) down to the space of catalyst bed. Thus, around ~325 min (oven temperature ~ 172 °C – Fig. 9a) gas temperature became noticeably higher than that of top. In further cooling, the curve of temperature at the top showed extremums, which testified to reaction zone shrinking down.

The experiment described above was repeated with just one modification – an insert made from quartz matt was installed above the catalyst bed. This prevented the reaction from occurring outside of the catalyst bed (Fig. 10). Temperature in the catalyst bed (top, bottom) and residual O_2 content changed during linear heating of the oven similarly to the previous experiment (Fig. 9), the difference being in the position of the "hot spot" – Fig. 10 shows it to remain the same when oven temperature became steady, unlike in Fig. 9a, i.e. the reaction did not spread out of the catalyst bed.

The phenomenon of H_2 oxidation reaction spreading outward into gas phase can be attributed both to surface defects in reactor walls and to the possible presence of catalyst dust particles on reactor walls.

3.6. Selectivity of CO-PROX over Rh-catalysts

Effects of temperature, Rh content in the catalyst, oxygen content in gas mixture (as the O_2/CO ratio) on residual contents of CO, O_2 are illustrated in Figs. 11 and 12. Data are obtained in gradual decrease in oven temperature after CSI was established at the switch from H_2 to $H_2/O_2/CO/N_2$.

As seen from Fig. 11, after the establishment of CSI a decrease in oven (catalyst) temperature to a certain level did not change the mode of reaction for Rh-catalysts: residual O_2 content stayed at a low level (below 100 ppm) at all contents of metal in the catalyst. As in the case of a Ru-catalyst (Fig. 5), a decrease in temperature favors a decrease in residual CO content, i.e. an increase in selectivity. Still, the curve of residual CO content for 0.2% Rh-catalysts lays

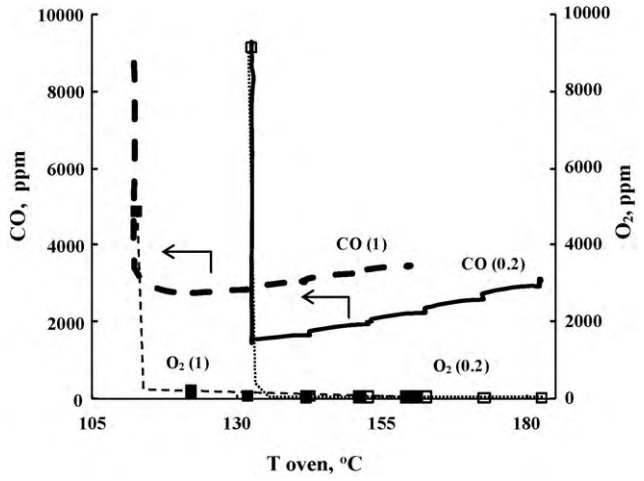

Fig. 11. Effects of temperature and metal content (the latter is reflected by the numbers in parentheses – 0.2 and 1 wt.%) on residual content of CO, O_2 in CO-PROX over Rh/Al_2O_3. Gas mixture composition, vol.%: O_2 – 0.97, CO – 0.97, H_2 – 62, N_2 – balance. GHSV 50 Nl (g cat.)$^{-1}$ h^{-1}.

below that for 1% Rh. Similar effect of metal content is noted for Ru-catalysts as well [16].

When the temperature was lowered below the aforementioned critical point (the lower the metal content, the higher this point), catalyst surface extinction happened and residual contents of O_2, CO grew rapidly (Fig. 11). Because the performance of a Rh-catalyst is favored by a growth (in certain range) in oxygen content [17], this can be used in bettering the selectivity. Corresponding data for 0.2% Rh/Al_2O_3 are shown in Fig. 12 (unlike for Fig. 11, for *x*-axis in Fig. 12 the gas temperature and not that of the oven was chosen).

An increase in O_2 content in gas mixture from 0.97 to 1.47 vol.% allowed to increase the selectivity: not only the residual CO content became lower in a comparable temperature range, but also the critical temperature of extinction did the same.

Let us note that at increased content of oxygen in gas mixture the residual CO content reached the minimum at ~30 ppm in the presence of quite significant CO_2 amount (Fig. 12). The presence of a small extremum around 110 °C on the curve of residual CO content for ratio $O_2/CO = 1.65$ (Fig. 12) can be attributed to superimposition of temperature and activity gradients along the catalyst bed.

Thus, it makes sense to research the optimal metal content for a set of reaction conditions (gas flow rate, gas composition).

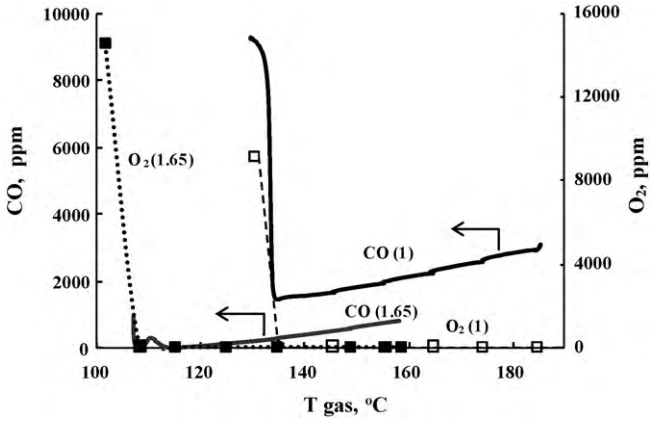

Fig. 12. Effects of temperature and O_2 content (O_2/CO ratio) in reaction mixture on residual content of CO, O_2 in CO-PROX over 0.2% Rh/Al_2O_3. For $O_2/CO = 1$ the gas mixture composition was (vol.%): O_2 – 0.97, CO – 0.97, H_2 – 62, N_2 – balance; for $O_2/CO = 1.65$, O_2 – 1.47, CO – 0.89, CO_2 – 23, H_2 – 71, N_2 – balance. GHSV 48 Nl (g cat.)$^{-1}$ h^{-1}.

4. Discussion

4.1. CSI mode

4.1.1. Conditions of catalyst surface ignition/extinction

Physical basis of CSI mode can be explained thus. When the constants of reaction rate grow with temperature exponentially, so does the heat flow generated by the reaction. At the same time, the heat flow leaving the reaction zone is in proportion (to some degree) to the difference between the reaction zone temperature and that of reaction gas entering the system. When the reaction zone temperature is increased above a certain value, a sudden shock to the macrokinetic mode of reaction may happen due to the discrepancy between the positive and negative heat flows noted in the beginning. This is observed as surface ignition – a temperature increase develops until the limit is met in influx of reactant molecules to the active centers of the surface. New steady regime is established where the reaction proceeds in external mass transfer control regime instead of the kinetic one (Transition into CSI mode followed by the establishment of steady-state CSI is shown, for example, in Figs. 2 and 3.).

Depending on the catalyst activity, reaction heat, etc., transition from the kinetic control regime into the external mass transfer control regime can proceed in time gradually or in a jump. Time required for the establishment of steady-state CSI depends on the strength of disturbance created and how close is the system to the critical parameters – these determine the difference between the flows of generated and dissipated heat in ignition and, accordingly, the rate of CSI spreading along the catalyst bed.

The possibility of jump-starting CO-PROX in CSI mode when the reaction gas is fed onto the catalyst at temperatures above the critical point of ignition (in this way, CSI is established quickly) is illustrated by Figs. 4 and 5. As seen from Fig. 5, after the reaction enters CSI mode, the latter is stable if the temperature stays above a certain level.

By varying the intensity of heat supply generated by reaction (i.e. by changing GHSV, reaction gas composition, oven temperature), it is possible to regulate the macrokinetic mode within certain limitations. After CSI has taken place, a decrease in oven temperature below the critical point of ignition does not lead to extinction in a certain temperature range – reaction is kept in so-called upper steady state (Fig. 6b) which corresponds to the external mass transfer control regime. Nevertheless, further decrease in oven temperature must result in the end in another disturbance – surface extinction, where reaction jumps back into the kinetic control regime (Figs. 5, 6, 11 and 12). Accordingly, this ignition/extinction situation results in a typical phenomenon of hysteresis (Fig. 6).

It should be noted that hysteresis phenomenon in CO-PROX has been reported before, for example in [34,35] for Cu-catalysts; still, in our opinion, it was interpreted incorrectly.

The lower the contribution of the reactor material and design to the heat dissipation or the higher the catalytic activity, the lower the critical ignition temperature. From another angle, the lower the content of the key reactant in reaction gas (in our case, oxygen – see Section 4.1.2) or the higher the heat capacity of gas mixture, the higher the critical ignition temperature.

Similar considerations can be made for critical temperature of extinction.

4.1.2. Key reactant in CO-PROX in CSI mode

It can be seen from data obtained (Figs. 2b, 3b, 4b, 5, 6a and 9b) that in steady-state CSI, residual oxygen content is quite low (does not exceed ~100 ppm). In this, when temperature is lowered without invoking the extinction (Figs. 5 and 6a), residual O_2 content stays about the same, but residual CO content changes substantially.

Thus, a conclusion can be made that it is oxygen which is the *key reactant* [24] defining the reaction transition into external mass transfer control regime. Of course, oxygen is also the key component in hydrogen oxidation transition into CSI mode (Figs. 7, 9 and 10).

4.1.3. Ignition and extinction features in the extension of catalyst bed

CSI mode can be entered or exited when temperature of "hot spot" in the catalyst bed reaches the *critical temperature* (of ignition or extinction correspondingly) [15,16,24].

When temperature is raised in the course of the process leading to CSI, also in the initial moment of transition mode, the "hot spot" is situated at the exit from the catalyst bed (the bottom), both in CO-PROX (Figs. 2c, 3c and 6a) and in H_2 oxidation (Figs. 9a and 10). Transition into the steady-state CSI mode is accompanied by the upstream drift of "hot spot".

In the course of extinction, "hot spot" drifts downstream until the bottom is reached (for example, Figs. 5 and 6a). Thus, in transition modes of both ignition and extinction there is a drifting zone within the catalyst bed, and the rate of its drift depends on certain conditions of the reaction.

As shown above, it is possible under certain conditions for hydrogen oxidation reaction in CO absence to spread into gas phase (see Section 3.5).

In steady-state CSI, CO-PROX proceeds at the entrance to the catalyst bed (the top), if there is no catalyst deactivation (Figs. 2–6 and 9). This presumes a substantial temperature gradient along the catalyst bed, so certain precautions must be applied to the experimental procedure. It should be said that it is not always that such precautions are considered by the researchers.

As a rule, in comparative estimations of catalytic activity in CO-PROX the comparisons are made of CO conversion dependences on temperature, or $T_{1/2}$ points (temperature values at which 50% CO conversion is achieved) [3]. Because CO conversion is determined by the temperature in "hot spot", it is important to perform the measurements in this spot and not in any other place for correct evaluation of activity dependence on temperature.

4.2. Effect of strong adsorption of a reactant on the conditions of catalyst surface ignition/extinction

In the case when just hydrogen and oxygen and not CO are present in reaction gas, hydrogen is easily oxidized over a metal surface (Pt, Rh), oxygen conversion being almost complete (Figs. 7, 9 and 10). In steady-state CSI, this occurs mostly in the "hot spot" which is situated at the top. When CO is added to the gas, extinction of hydrogen oxidation can be observed due to preferable CO adsorption over active centers of metal. Catalytic activity can be restored in the reaction gas free from CO. This result is in agreement with data [36] where a flow of CO/Ar/He was switched to O_2/Ar/He over 2.9% Pt/Al_2O_3 at 300 K, which led to quick disappearance (in dozens of seconds) of linear CO forms due to formation of CO_2.

It is evident that the rate of catalyst deactivation by CO depends on content of metal in the catalyst, temperature, concentrations of CO and O_2, and on the gas flow rate. In the experiment depicted in Fig. 7e, "quick" stage of deactivation, the downstream drift of "hot spot", took as little as ~0.1 min. At higher temperatures, this stage can take more time. We believe that "rapid" deactivation (in fact, a matter of a few minutes) of 5% Pt/γ-Al_2O_3 observed in [37] at 90 °C (loading 50 mg, GHSV 190,000 h^{-1}) which occurred when hydrogen was switched to the mixture of the composition (vol.%): H_2 – 45, CO – 1, O_2 – 1, He – balance, had at its basis strong adsorption of CO and not the formation of carbonaceous deposits as thought by authors of that work.

As shown above, strong adsorption of CO over metal surface creates a shortage of free surface, thus lowering catalytic activity and accordingly, the amount of heat generated by the reaction. One possible consequence of these effects would be slow continuous change in catalyst temperature and residual O_2 content at constant oven temperature over time (Fig. 8).

This slow deactivation is confirmed by data on CO-PROX over Pt [3,13] and Pt, Rh [9]. In [13], for 5% Pt/γ-Al_2O_3 at 65 °C slow slight decrease in conversion of CO, O_2 was observed for ~80 h. In [3], deactivation of a Pt-catalyst occurred, as a rule, within 2 h of reaction gas containing CO, O_2, H_2 being fed onto the catalyst. Further deactivation gave about 5% loss of activity during the next 10 h. Stability of Pt-, Rh-catalysts in CO-PROX was studied in [9] in 33 h runs. It was found that CO conversion decreased exponentially in time: for Rh – by 70% (at 150 °C) and 30% (at 250 °C); for Pt – by 50% (at 200 °C).

As follows from the discussion above, deactivating effect of CO on Pt-, Rh-catalysts can be decreased by increasing O_2 content in reaction gas and/or reaction temperature.

Combination of strong exothermicity of H_2, CO oxidation and strong CO adsorption in continuous layer of catalyst can lead to appearance of oscillations, as shown in [31] for 0.2% Rh-catalyst.

For Ru-catalysts, the decisive factor of deactivation is strong oxygen adsorption [16,32] which can lead also to complicated transition modes up to appearance of oscillations with periods of dozens minutes [32]. As in the case of Ru-catalysts, hydrogen makes substantial positive effect on CO oxidation over Au-catalysts.

5. Conclusions

(1) Preferential oxidation of CO (CO-PROX) can be realized in a special macrokinetic mode of catalyst surface ignition (CSI). This is an external mass transfer control regime on the key reactant (oxygen in the case of CO-PROX).
(2) Reaction transition into CSI mode at the increase in oven temperature is manifested in the catalyst overheat at the exit from the catalyst bed, after which the CSI mode spreads upstream.
(3) Both surface ignition and extinction can be observed through variation of oven temperature. In this, curves of the catalyst bed temperature and of residual contents of CO, O_2 reveal hysteresis depending on temperature of incoming gas.
(4) Over Pt-, Rh-catalysts carbon monoxide can show deactivating effect on CO-PROX due to its strong adsorption over these metals, even in the presence of hydrogen.
(5) In CO absence, H_2 is easily oxidized over Pt, Rh even at temperatures close to the room one. Reaction proceeds in CSI mode in the frontal layer; it is possible for reaction to spread into gas phase if the latter is free from space-filling obstacles.
(6) A prolonged decrease in residual CO content was observed after the establishment of steady-state CSI over 1% Rh/Al_2O_3. This is probably connected to the processes of metal crystallites restructuring.
(7) Effects of temperature, oxygen content in gas and metal content (for Rh-catalysts) are investigated. It is shown that an increase in oxygen content, a decrease in temperature and a decrease in metal content from 1 to 0.2 wt.% all favor decreased residual content of CO.

Acknowledgements

Authors would like to thank their colleagues I.N. Zavalishin and P.V. Samokhin for useful discussion.

This work has been done with the support of Russian Foundation for Basic Research (Grant Nos. 06-03-32848, 09-03-00226).

References

[1] M.L. Brown, A.W. Green, US Patent 3,088,919 (7 May 1963).
[2] J.G.E. Cohn, US Patent 3,216,783 (9 November 1965).
[3] M.J. Kahlich, H.A. Gasteiger, R.J. Behm, J. Catal. 171 (1997) 93–105.
[4] P.V. Snytnikov, V.A. Sobyanin, V.D. Belyaev, P.G. Tsyrulnikov, N.B. Shitova, D.A. Shlyapin, Appl. Catal. A 239 (2003) 149–156.
[5] C.D. Dudfield, R. Chen, P.L. Adcock, J. Power Sources 86 (2000) 214–222.
[6] C.D. Dudfield, R. Chen, P.L. Adcock, J. Power Sources 85 (2000) 237–244.
[7] I. Rosso, M. Antonini, C. Galletti, G. Saracco, V. Specchia, Top. Catal. 30–31 (2004) 475–480.
[8] A. Manasilp, E. Gulari, Appl. Catal. B 37 (2002) 17–25.
[9] Y.-F. Han, M.J. Kahlich, M. Kinne, R.J. Behm, Appl. Catal. B 50 (2004) 209–218.
[10] Y.-F. Han, M. Kinne, R.J. Behm, Appl. Catal. B 52 (2004) 123–134.
[11] S.H. Oh, R.M. Sinkevitch, J. Catal. 142 (1993) 254–262.
[12] I. Rosso, C. Galletti, G. Saracco, E. Garrone, V. Specchia, Appl. Catal. B 48 (2004) 195–303.
[13] G. Avgouropoulos, T. Ioannides, Ch. Papadopoulou, J. Batista, S. Hocevar, H.K. Matralis, Catal. Today 75 (2002) 157–167.
[14] A.Ya. Rozovskii, G.I. Lin, M.A. Kipnis, P.V. Samokhin, E.A. Volnina, I.A. Belostotsky, G.M. Grafova, I.N. Zavalishin, Top. Catal. 42–43 (2007) 437–441.
[15] A.Ya. Rozovskii, M.A. Kipnis, E.A. Volnina, G.I. Lin, P.V. Samokhin, Kinet. Catal. 48 (2007) 701–710.
[16] A.Ya. Rozovskii, M.A. Kipnis, E.A. Volnina, P.V. Samokhin, G.I. Lin, Kinet. Catal. 49 (2008) 92–102.
[17] C. Galletti, S. Fiorot, S. Specchia, G. Saracco, V. Specchia, Top. Catal. 45 (2007) 15–19.
[18] E. Quinet, F. Morfin, F. Diehl, P. Avenier, V. Caps, J.-L. Rousset, Appl. Catal. B 80 (2008) 195–201.
[19] C. Galletti, S. Fiorot, S. Specchia, G. Saracco, V. Specchia, Chem. Eng. J. 134 (2007) 45–50.
[20] I. Rosso, C. Galletti, S. Fiorot, G. Saracco, E. Garrone, V. Specchia, J. Porous Mater. 14 (2007) 245–250.
[21] S. Specchia, C. Galletti, S. Fiorot, G. Saracco, V. Specchia, ECS Trans. 5 (2007) 677–685.
[22] C. Galletti, S. Specchia, G. Saracco, V. Specchia, Ind. Eng. Chem. Res. 47 (2008) 5304–5312.
[23] C. Galletti, S. Specchia, G. Saracco, V. Specchia, Chem. Eng. J. 154 (2009) 246–250.
[24] D.A. Frank-Kamenetskii, Diffusion and Heat Transfer in Chemical Kinetics, Plenum Press, New York, 1969.
[25] J.T. Kiss, R.D. Gonzalez, J. Phys. Chem. 88 (1984) 898–904.
[26] K. Arnby, A. Törncrona, B. Andersson, M. Skoglundh, J. Catal. 221 (2004) 252–261.
[27] K. Arnby, J. Assiks, P.-A. Carlsson, A. Palmqvist, M. Skoglundh, J. Catal. 233 (2005) 176–185.
[28] M. Skoglundh, P. Thormählen, B. Andersson, Top. Catal. 30–31 (2004) 375–381.
[29] M.M. Schubert, M.J. Kahlich, H.A. Gasteiger, R.J. Behm, J. Power Sources 84 (1999) 175–182.
[30] P.V. Snytnikov, V.D. Belyaev, V.A. Sobyanin, Kinet. Catal. 48 (2007) 93–102.
[31] M.A. Kipnis, E.A. Volnina, Kinet. Catal. 51 (2010) 279–287.
[32] A.Ya. Rozovskii, M.A. Kipnis, E.A. Volnina, P.V. Samokhin, G.I. Lin, M.A. Kukina, Kinet. Catal. 50 (2009) 691–704.
[33] E. Quinet, L. Piccolo, F. Morfin, P. Avenier, F. Diehl, V. Caps, J.-L. Rousset, J. Catal. 268 (2009) 384–389.
[34] M. Manzoli, R. Di Monte, F. Boccuzzi, S. Coluccia, J. Kaspar, Appl. Catal. B 61 (2005) 192–205.
[35] J.B. Wang, S.-C. Lin, T.-J. Huang, Appl. Catal. A 232 (2002) 107–120.
[36] A. Bourane, D. Bianchi, J. Catal. 209 (2002) 114–125.
[37] A. Sirijaruphan, J.G. Goodwin Jr., R.W. Rice, J. Catal. 221 (2004) 288–293.